Development/Plasticity/Repair

Mutations in *deadly seven/notch1a* Reveal Developmental Plasticity in the Escape Response Circuit

Katharine S. Liu,[1]* Michelle Gray,[2,3]* Stefanie J. Otto,[1] Joseph R. Fetcho,[1] and Christine E. Beattie[2,3,4]

[1]Department of Neurobiology, State University of New York at Stony Brook, Stony Brook, New York 11794, [2]Center for Molecular Neurobiology, [3]Molecular, Cellular, and Developmental Biology Program, and [4]Department of Neuroscience, The Ohio State University, Columbus, Ohio 43210

The relatively simple neural circuit driving the escape response in zebrafish offers an excellent opportunity to study properties of neural circuit formation. The hindbrain Mauthner cell is an essential component of this circuit. Mutations in the zebrafish *deadly seven/notch1a* (*des*) gene result in supernumerary Mauthner cells. We addressed whether and how these extra cells are incorporated into the escape-response circuit. Calcium imaging revealed that all Mauthner cells in *des*^{b420} mutants were active during an elicited escape response. However, the kinematic performance of the escape response in mutant larvae was very similar to wild-type fish. Analysis of the relationship between Mauthner axon collaterals and spinal neurons revealed that there was a decrease in the number of axon collaterals per Mauthner axon in mutant larvae compared with wild-type larvae, indicative of a decrease in the number of synapses formed with target spinal neurons. Moreover, we show that Mauthner axons projecting on the same side of the nervous system have primarily nonoverlapping collaterals. These data support the hypothesis that excess Mauthner cells are incorporated into the escape-response circuit, but they divide their target territory to maintain a normal response, thus demonstrating plasticity in the formation of the escape-response circuit. Such plasticity may be key to the evolution of the startle responses in mammals, which use larger populations of neurons in circuits similar to those in the fish escape response.

Key words: **hindbrain; behavior; calcium imaging; mutant analysis; Mauthner cell; *notch1a*; axon collaterals**

Introduction

Establishing functional neural circuits involves numerous developmental processes, including the generation of the correct cell number and cell type and the establishment of appropriate connections between cells. Mutations that alter these processes have the potential to disrupt the relationship between cell types in a circuit and can compromise downstream behavior, unless the animal can adapt to such changes. Zebrafish offer several advantages as a model system for studying the impact of mutations on circuitry and behavior. In aquatic vertebrates, such as fish and premetamorphic amphibians, relatively simple neural circuits control fundamental motor behaviors. These circuits often have relatively few cells, and, in some cases, it is possible to identify individual cells and link them to a behavior. This is particularly true in the zebrafish hindbrain, in which there is an array of morphologically distinct reticulospinal neurons with characteristic cell body locations and stereotyped axon projections (Metcalfe et al., 1986). The largest of these, the Mauthner cell, is present bilaterally in rhombomere segment 4 and sends its axon across the midline where it descends to make monosynaptic connections with contralateral interneurons and motoneurons along the length of the spinal cord (Faber and Korn, 1978). Experiments in both zebrafish and goldfish have shown that activation of the Mauthner cell initiates a coordinated bend away from the direction of the stimulus, allowing the animal to swim away from a perceived threat (Zottoli, 1977). Two homologous reticulospinal neurons are also involved in the escape circuitry (Liu and Fetcho, 1999); however, activation of the Mauthner cell is sufficient to trigger the behavior (Zottoli, 1977; Eaton et al., 1981; Nissanov et al., 1990), demonstrating a one-to-one correlation between Mauthner cell firing and the escape response.

Mutations in the *des*/*notch1a* gene (van Eeden et al., 1996; Holley et al., 2002) result in supernumerary Mauthner cells (Gray et al., 2001). We took advantage of this defect to ask how the nervous system responds to specific alterations in a defined neural circuit. We found that all Mauthner cells present in *des*^{b420} mutants are active during an escape response. Quantitation of kinematics of the escape movements reveals little difference between wild-type and mutant larvae. However, analysis of Mauthner axons in two *des* alleles reveals a dramatic decrease in the number of axon collaterals compared with wild-type Mauthner axons. In addition, the number of Mauthner cells is inversely proportional to the number of axon collaterals per Mauthner cell. Mauthner axons extending down the same side of the spinal cord

Received May 1, 2003; revised July 3, 2003; accepted July 16, 2003.

This work was supported by a postdoctoral fellowship from the Helen Hay Whitney Foundation (K.S.L.), National Institute of Neurological Disorders and Stroke Grant F31 NS11056-01A1 (M.G.), National Institutes of Health Grant NS26539 (J.R.F.), and National Science Foundation Grant IBN-9817076 (C.E.B.). We thank the support staff of our zebrafish facilities for maintaining fish lines, and Cecilia Moens (Fred Hutchinson Cancer Reserach Center, Seattle, WA) for helpful comments on this manuscript. The 3A10 monoclonal antibody, developed by Thomas M. Jessell and Jane Dodd (Columbia University, New York, NY), was obtained from the Developmental Studies Hybridoma Bank, developed under the auspices of the National Institute of Child Health and Human Development, and maintained by The University of Iowa Department of Biological Sciences.

*K.S.L. and M.G. contributed equally to this work.

Correspondence should be addressed to Christine E. Beattie, Department of Neuroscience, Center for Molecular Neurobiology, 115 Rightmire Hall, 1060 Carmack Road, Columbus, OH 43210. E-mail: beattie.24@osu.edu.

 0270-6474/03/238159-08$15.00/0

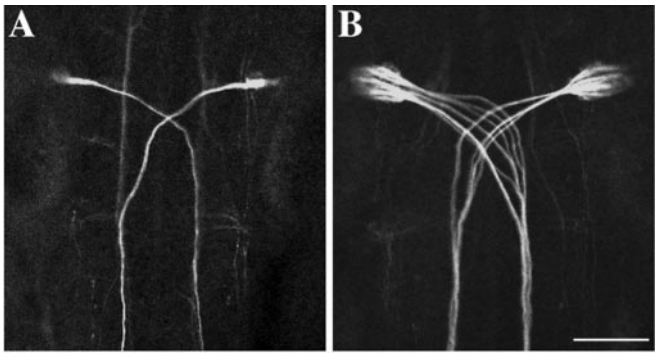

Figure 1. *des* mutants have supernumerary Mauthner cells. *A*, *B*, Mauthner cells in a 30 hr wild-type (*A*) and des^{b420} (*B*) mutant embryo as revealed by 3A10 antibody labeling and confocal microscopy. Dorsal views with anterior to the top. Scale bar, 40 μm.

primarily have collaterals in different positions, suggesting that contacts are being formed on nonoverlapping populations of cells. These data suggest that the formation of the escape-response circuit is highly adaptive and can compensate for supernumerary Mauthner cells by regulating the number of synapses formed on target cells in the spinal cord, thus maintaining a normal escape response.

Materials and Methods

Fish care and identification. Mutant embryos and larvae were obtained from a laboratory breeding stock of heterozygous adult fish. Homozygote mutants were obtained from natural mating of heterozygous adults and were identified by their somitic defect that results in irregular muscle patterns. Both the b420 and tp37 allele carry ethylnitrosourea-induced mutations (van Eeden et al., 1996; Gray et al., 2001). Larval zebrafish refer to fish at 3–6 d post-fertilization (dpf).

Whole-mount antibody labeling. Whole-mount antibody labeling with 3A10 antibody (1/10; Developmental Studies Hybridoma Bank, University of Iowa, Iowa City, IA) and acetylated tubulin (1/400; Sigma, St. Louis, MO) were processed as described by Gray et al. (2001).

Retrograde labeling of calcium green dextran. Larval zebrafish were anesthetized with 0.02% 3-aminobenzoic acid ethyl ester (MS222, tricaine). The targeted cells were retrogradely labeled by pressure injection via a glass microelectrode of a 50% solution of calcium green dextran [10,000 molecular weight (MW); Molecular Probes, Eugene, OR) in 10% HBSS into the caudal spinal cord (Fetcho and O'Malley, 1995). Injections were targeted to the ventral cord to selectively label Mauthner cells and their homologs without disrupting more dorsal sensory pathways. After injection, fish were allowed to recover in 10% HBSS. Carefully done, such injections do not alter the behavior of the fish and therefore are unlikely to have altered the normal activity in the labeled cells (Liu and Fetcho, 1999).

Calcium imaging. Calcium imaging was performed as described previously (Fetcho and O'Malley, 1995; O'Malley et al., 1996). Nine to ten hours after labeling, fish were briefly anesthetized in tricaine, placed on a cover glass in a Petri dish, embedded on their backs in a thin layer of 1.2% agar, and screened under confocal microscopy. Confocal images were obtained by looking into the head of the intact fish using a Zeiss (Thornwood, NY) inverted microscope with a 63× water objective and a Zeiss laser-scanning confocal imaging system. Mauthner cells were identified by their highly characteristic morphology and position (Metcalfe et al., 1986).

Escapes were elicited by a small tap from a polished glass probe attached to a piezoelectric crystal. The stimulus (tap) strength could be controlled by the amount of voltage applied to the crystal. Taps given to the head were aimed at the ear of the animal, ipsilateral to the group of cells under observation. Taps given to the tail were aimed rostral of the injection site and ipsilateral to the observed cells.

The fluorescence intensities of the cells were monitored by collecting a baseline series of images of a group of labeled Mauthner cells at 300 msec intervals before delivering the stimulus. To avoid false positives resulting from the cells moving to a brighter plane of focus, we started with the brightest plane of focus, optimizing for one cell at a time per trial. Although the optimized cell increased in fluorescence intensity, in most cases, the surrounding Mauthner cells could be seen to brighten as well.

High-speed recording of behavior. High-speed recording was performed as described previously (Liu and Fetcho, 1999), except that a different escape-inducing stimulus was used. Test larvae were placed into individual Petri dishes (3.5 cm) and assigned a number designation. Escape responses were recorded under a high-speed camera that captured images digitally at 1000 frames per second connected to a dissecting microscope. Escape responses were elicited by a small tap to either the head or tail of the fish delivered by a small, polished glass probe. A successful escape trial was recorded from the time the probe visually contacted the fish to when the fish swam to the edge of the field of view.

Fish were tapped on the left side of the head for the first trial, on the right side of the head for the second trial, and then the left side of the tail for the third trial, and so on. Stimuli to the head were directed at the ear, whereas stimuli to the tail were directed caudal to the anal pore. All fish in the group were tested for the same quadrant before moving on to the next trial, resulting in each fish resting for an average of 20 min between trails, and each fish was not presented with a stimulus in the same quadrant for well over 1 hr. Such delays should prevent habituation, fatigue, etc. On occasion, a fish failed to respond to the stimulus, gave a premature response, or turned slightly on its side. Only responses that occurred after the stimulus were deployed, and in which the fish remained upright throughout the initial bend were kept digitally. Because des^{b420} homozygotes do not develop a swim bladder, we chose to collect our trials at 3 dpf, when neither wild-type larvae nor des^{b420} larvae have swim bladders.

Data analysis. Analyses of the recorded movement data were done as described previously (Liu and Fetcho, 1999). Several kinematic parameters of the initial turn of the escape response were selected for analysis: latency to its initiation (time from the contact of glass probe to the beginning of movement), the maximum angle of the turn, its peak angular velocity, and its duration (time from beginning of movement to maximum angle). Movements were then analyzed for these kinematic parameters using a specialized program written in Labview (National Instruments, Austin, TX). The analysis was automated, the image of the fish was thresholded, and the silhouette of the fish was used to determine the location of the rostral midline. The midline from each successive frame was plotted to give a representation of the animal's movements. The program calculated the angle between the position of the midline in successive frames and its original position and also provided other kinematic data, such as the angular velocity. These parameters were then statistically compared using ANOVA (SuperAnova; Abacus Concepts, Berkeley, CA).

Single Mauthner axon labels. Mauthner axons of 3 dpf larvae, anesthetized in tricaine, were retrogradely labeled by pressure injection into the spinal cord using a glass electrode filled with 5% lysinated rhodamine dextran (10,000 MW) (all fluorescent dextrans used in this study were obtained from Molecular Probes) at approximately hemisegment 25. After labeling, larvae were allowed to recover for 24 hr. Because of the difficulty in resolving multiple fluorescent-labeled axons in des^{b420} mutants, only larvae with one labeled Mauthner axon were scored. Collaterals were imaged and counted under confocal microscopy (63×) over a three-somite length corresponding to three spinal cord hemisegments. The total number of Mauthner cells present on the corresponding side of the hindbrain was quantitated on a Zeiss Axioplan compound microscope under transmitted light (40×).

Dual-color Mauthner axon labels. Mauthner cells of 4 dpf larvae, anesthetized in tricaine, were retrogradely labeled by pressure injection into the spinal cord using a glass electrode filled with 10% fluorescein dextran (3000 MW). After a recovery of 48 hr, fish were screened for labeled Mauthner cells. These fish were anesthetized again, placed on a cover glass in a Petri dish, and embedded upright (dorsal side up) in a layer of 1.2% agar. Mauthner cells were targeted for electroporation under FITC fluorescence. For electroporation, thin-walled filamented glass microelectrodes backfilled with either 10% rhodamine dextran (3000 MW) or

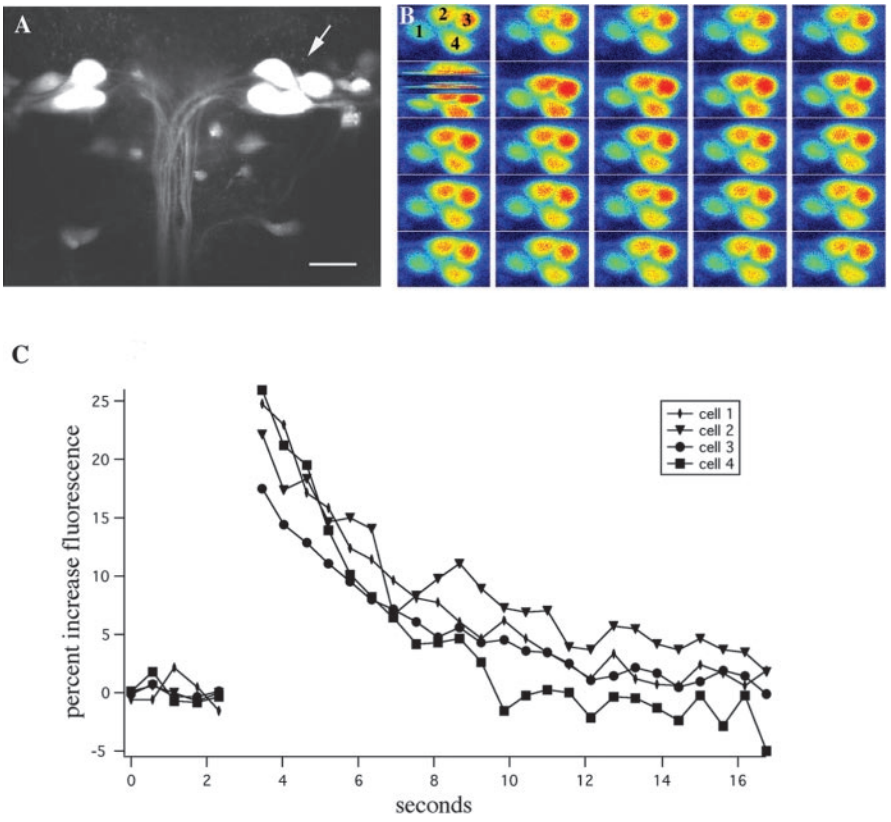

Figure 2. Mauthner cells in *des* mutants are active during an escape response. A calcium-imaging trial of a des^{b420} mutant is shown. *A*, Mauthner cells in mutant larvae were backfilled with the fluorescent dye, calcium green dextran, at 4 dpf and imaged on confocal microscopy with a 63× objective. *B*, For quantification purposes, Mauthner cells on the right side of the hindbrain (*A*, arrow) were numbered 1 through 4. Fluorescence intensities were presented in pseudocolor with red being the brightest. In this trial, the plane of focus was optimized for cell 3. However, as is typically the case, all four cells were noticeably brighter after the escape when compared with the baseline of frames collected before the stimulus. The distortion in frame 6 indicates movement of the fish in response to a tap on the tail. Frames are ordered from left to right with 578 msec between frames. *C*, Quantification of the increase in fluorescence intensities. The fluorescence intensities for each cell (1–4) were plotted for each frame. The *y*-axis shows the normalized intensities ($\Delta F/F$). The *x*-axis shows the time in seconds. Scale bar, 30 μm.

10% Alexa 647 (10,000 MW) were used to electroporate single Mauthner cells (Haas et al., 2002). Once the electrode was in position next to a Mauthner cell body, two to three trains of pulses (train width, 3 sec; pulse duration, 1 msec; pulse period, 10 msec; frequency, 100 pulses/sec; amplitude, 10 V) were applied using an A-M systems-isolated pulse stimulator (model 2100; A-M Systems, Carlsburg, WA) and a custom-built electroporation apparatus. The number of pulse trains (usually 2 or 3) was determined visually by monitoring the extent of cell filling under fluorescence. Once a single Mauthner cell was filled with dye (either rhodamine or Far Red), the positive pressure was reapplied to the electrode as it was moved out of the head. A second microelectrode, this time filled with the other dye (i.e., Far Red if rhodamine was used first), was positioned in the head adjacent to a second fluorescein-labeled Mauthner cell located within the same cluster of cells and electroporated using the method described above. After electroporation, the fish were reembedded on their sides in 1.2% agar, in tricaine, and imaged on a Zeiss 510 confocal laser scanning microscope using a Zeiss 63× water objective to image collaterals.

Results

The escape response circuit in des^{b420} mutants

The neural circuit driving the escape response in zebrafish is mediated by a defined set of neurons. Sensory input from the trigeminal (V) cranial nerve, acoustic (VIII) cranial nerve, and lateral line contact the Mauthner cell lateral dendrite (Kimmel et al., 1981,1990). Mauthner cells extend axons down the spinal cord and contact primary motoneurons and interneurons (Fetcho and Faber, 1988). We have shown previously that des^{b420} mutants have a restricted neurogenic phenotype (Gray et al., 2001). Wild-type animals possess a single pair of Mauthner cells located in hindbrain rhombomere 4 (Fig. 1*A*). In des^{b420} mutants, however, the Mauthner cell is variably increased in number with between three and eight cells present on each side representing a 4.8-fold increase in Mauthner cell number (Fig. 1*B*) (Gray et al., 2001). There is also an ~19% increase in primary motoneurons in des^{b420} mutants, whereas all other cells in the escape-response circuit appeared unaffected (Gray et al., 2001). Mauthner axons in *des* mutants cross the midline and then extend posteriorly within the contralateral side of the spinal cord, consistent with what is seen in wild-type larva (Fig. 1). Thus, the escape-response circuit in des^{b420} mutants is characterized as having a dramatic increase in Mauthner cell number without major alterations in cell body location or axon projections and with a small or no increase in the other cell types participating in the circuit.

Supernumerary Mauthner cells are active during the escape response

The presence of excess Mauthner cells in des^{b420} mutants prompted us to ask whether all of these cells participated in the escape response. Taking advantage of the transparency of zebrafish larvae, we used optical imaging of calcium-dependent fluorescent indicators to monitor the activity of several cells simultaneously (O'Malley et al., 1996). This technique was used to determine the activity patterns of supernumerary Mauthner cells during escape responses elicited by a tap with a glass probe, deflected by a piezoelectric crystal. Although some taps were administered to the head, we concentrated on escapes elicited by taps to the tail, because the Mauthner cell is known to play a larger role in these responses (O'Malley et al., 1996; Liu and Fetcho, 1999).

Data were collected from 21 escape trials (17 to tail and 4 to head) from six fish. Figure 2 shows an example of a calcium-imaging trial. In this case, four cells were labeled on the side being imaged (Fig. 2*A*, arrow), and the change in fluorescence intensities was quantified (Fig. 2*B*,*C*). Because of potential movement artifacts, each calcium-imaging trial began at the brightest plane of focus for the cell of interest (Fetcho and O'Malley, 1995). Because the supernumerary Mauthner cells do not all lie in the same plane of focus, the focal plane was altered in consecutive trials within the same animal, each time optimizing for a particular cell (Fig. 2*B*, cell 3). In most cases, even the surrounding cells outside the focal plane gave robust responses. In every case, the optimized cell displayed a significant increase in fluorescence. All labeled Mauthner cells examined were activated during escape. These data suggest that all supernumerary Mauthner cells in des^{b420} mutants are integrated into the escape circuit.

The observation that all of the Mauthner cells responded to

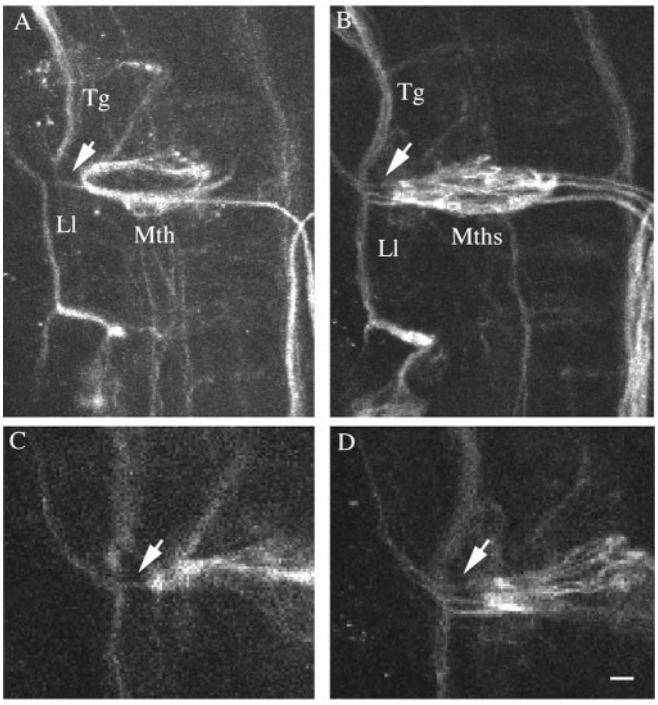

Figure 3. Mauthner cell lateral dendrites in *des* mutants are in close apposition to sensory nerves. *A–D*, Seventy-two hour wild-type (*A*, *C*) and mutant (*B*, *D*) embryos were labeled with 3A10 antibody and analyzed by confocal microscopy. The trigeminal (Tg) and lateral line (Ll) nerves extend perpendicular to the Mauthner cell (Mth) and are closely juxtaposed to Mauthner cell lateral dendrites (arrow). *A* and *B* are the left sides of merged sections of wild-type and mutant embryos; *C* and *D* are single optical sections through the wild-type and mutant embryo shown in *A* and *B*. All images are dorsal views with anterior to the top. Scale bar, 35 μm

the stimulus might be a consequence of a strong stimulus that was suprathreshold for all cells, or it might be a result of mutual excitation among the cells via gap junctions or other synaptic interactions. To attempt to distinguish between these two possibilities, we repeated the calcium-imaging experiments while lowering the stimulus intensity to threshold, which is the intensity at which the fish escapes 50% of the time when presented with the stimulus. If Mauthner cells were independently activated by the sensory inputs, we might expect that near threshold for the behavior, some cells would fire and not others because of slight differences in the level of sensory input or threshold of the cells that would bring some cells to threshold and not others. The threshold stimulus intensity was determined for a mutant fish by varying the tap strength to find a strength at which the fish escaped to ~50% of the taps. Once the threshold was determined for a particular fish, the responses of the Mauthner cells to a stimulus at threshold were examined in that fish ($n = 3$ fish). As before, all labeled Mauthner cells were activated during these escapes to a threshold stimulus. These data suggest that all the Mauthner cells are firing together even at threshold, supporting the hypothesis that some interactions between the cells (e.g., via gap junctions or chemical synapses) assure that they function together.

Mauthner cells are contacted presynaptically on the Mauthner cell lateral dendrite by the trigeminal, acoustic, and lateral line nerves (Kimmel et al., 1990). We used confocal microscopy to examine the spatial relationship between these nerves and Mauthner cell lateral dendrites in *des*^{b420} mutants. Mauthner cell bodies in *des*^{b420} mutants are compact and assume the position of wild-type Mauthner cells. We found that all of the Mauthner cell lateral dendrites in *des*^{b420} mutants spatially overlapped with the three sensory nerves, with the trigeminal and lateral line nerves as the most easily observed (Fig. 3). Because of the small axon diameter of these nerves, we were unable to visualize singular axon collaterals; however, the close apposition of the presynaptic nerves and the postsynaptic lateral dendrite shows that all Mauthner cells in *des*^{b42} mutants could potentially receive sensory input. This lends support to the hypothesis that all of the Mauthner cells receive some direct input during an escape response.

Escape performance is similar in wild-type and *des*^{b420} mutant larvae

The Mauthner cell is known to play a major role in escape performance, particularly in tail-elicited escapes (Liu and Fetcho, 1999). The calcium-imaging data revealed that all Mauthner cells were active during an escape response, suggesting that *des*^{b420} mutants might exhibit abnormal escape responses. One prediction is that the escape response in mutants would be exaggerated in terms of the speed of the escape (angular velocity) caused by the extra Mauthner cells. Moreover, because there are multiple Mauthner cells present in mutants compared with the single Mauthner cell in wild type, this might alter the time to respond to the stimuli (latency to response).

To compare the escape performance of *des*^{b420} mutants with wild-type animals, we captured escape responses with a high-speed (1000 frames per second) digital camera (Fig. 4) and compared several kinematic parameters (Table 1). Data were collected from two groups: 20 trials (5 each to left head, right head, left tail, and right tail) from six *des*^{b420} mutants and five wild-type animals, and 20 trials from six *des*^{b420} mutants and four wild-type siblings. The trials were analyzed via a computer program written to automatically extract several parameters for each frame (Liu and Fetcho, 1999).

Surprisingly, performance measurements that assess the function of Mauthner cells in the escape response were primarily unaffected in *des*^{b420} mutant larvae compared with wild-type larvae (Table 1). In particular, the peak angular velocity was unaffected ($p > 0.05$), suggesting that performance was not increased by the presence of extra Mauthner cells. The latency to respond was also not significantly different between mutant and wild-type larvae for both head- and tail-elicited responses ($p > 0.05$). Previous Mauthner cell lesion studies showed no effect on turn angle after killing the Mauthner cell and its hindbrain homologues (Liu and Fetcho, 1999). Turn angle was significantly different between mutant and wild-type larvae for the head-elicited response ($p < 0.001$) but was not significantly different for the tail response in which the Mauthner cell is normally activated independently of its hindbrain homologues ($p > 0.05$). This suggests that some of the other defects in *des* mutants could be affecting this parameter in head-elicited responses. The peak turn duration was statistically longer in mutant compared with wild-type larvae ($p < 0.001$) in tail-elicited but not head-elicited responses. Thus, six of eight comparisons of the movements showed no differences between mutant and wild-type larvae, and these unchanged parameters included two (latency and peak angular velocity) in which the Mauthner cell is thought to play a key role on the basis of previous lesion experiments. Although *des* mutants have defects in somite and myotome formation (van Eeden et al., 1996; Gray et al., 2001; Holley et al., 2002), this does not appear to dramatically affect the escape response.

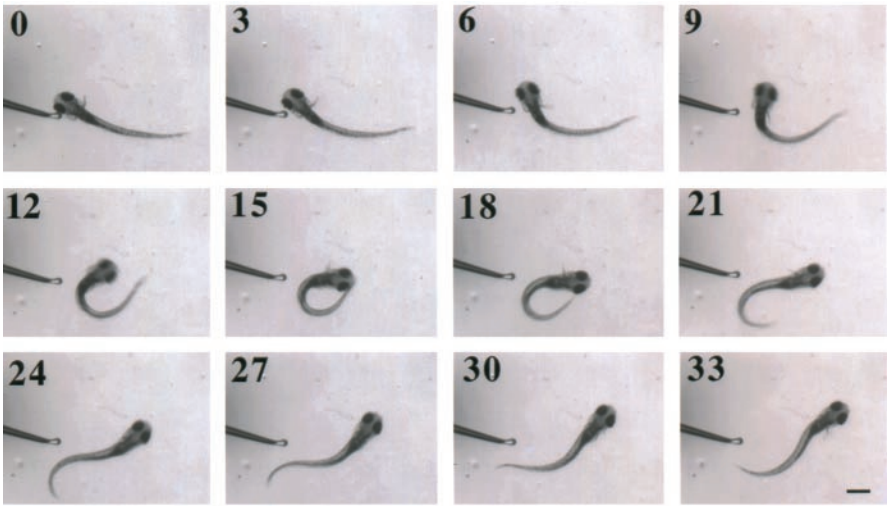

Figure 4. *des*^{b420} mutant larvae exhibited primarily normal escape responses. A tap with a small polished glass probe elicited escapes. In this trial, the tap was delivered to the left side of the head (bottom left-hand corner). Images were captured at 1000 frames per second. Every third frame (msec) is shown, starting at the initiation of the response (frame 0). After the start of movement, peak turn angle is reached at 15 msec (15). For an example of a wild-type escape response, see Liu and Fetcho (1999). Scale bar, 550 μm.

Mauthner axons in *des* mutants have fewer axon collaterals

Despite the presence of supernumerary Mauthner cells contributing to the circuit, the escape response in *des*^{b420} mutants was relatively unaffected. One explanation for this finding is that each Mauthner cell could be playing a correspondingly smaller role in mediating the escape behavior. Mauthner cells drive the escape response by synapsing directly onto contralateral interneurons and motoneurons in the spinal cord via axon collaterals (Fetcho and Faber, 1988). To determine the relationship between Mauthner cells and downstream spinal neurons, we quantitated the number of axon collaterals present on individual Mauthner axons in wild-type and mutant larvae over a defined length of axon corresponding to three spinal cord hemisegments. Single Mauthner axons in wild types and *des* mutants were back-labeled from the spinal cord in 3 dpf larvae and analyzed under confocal microscopy at 4 dpf. Collaterals were positively identified by their knob-like appearance as reported previously (Gahtan and O'Malley, 2003). Axon collateral counts at 4 dpf revealed that individual Mauthner axons in *des*^{b420} mutants had a dramatic decrease in axon collaterals compared with individual wild-type Mauthner axons (Fig. 5*A*,*B*; Table 2). Mauthner cells in *des*^{b420} mutants had an ~78% decrease in the number of axon collaterals compared with wild-type Mauthner axons (Fig. 5*C*; Table 2).

These data suggest that there is a relationship between the number of axon collaterals and the number of Mauthner cells; that is, when more Mauthner cells are present, there are fewer axon collaterals per Mauthner axon. To examine the relationship between Mauthner cell number and the number of axon collaterals per Mauthner axon, we analyzed *des*^{tp37} mutants (van Eeden et al., 1996), which have a less dramatic increase in Mauthner cells (Gray et al., 2001). Whereas *des*^{b420} mutants have an ~4.8-fold increase in Mauthner cells when compared with wild-type embryos, *des*^{tp37} mutants have an ~3.6-fold increase in Mauthner cells (Gray et al., 2001) (Table 2). Quantitation of axon collaterals in *des*^{tp37} mutants revealed an ~56% decrease in the number of collaterals per Mauthner axon, a less dramatic decrease than that seen in the b420 mutant allele but still significantly fewer collaterals than seen on wild-type Mauthner axons (Table 2). These data are consistent with an inverse relationship between the number of Mauthner cells and the number of collaterals per Mauthner axon.

When there is a greater number of Mauthner cells, each Mauthner axon has fewer collaterals, suggesting that the Mauthner axons are dividing their synaptic targets in the spinal cord. If this were the case, we would expect Mauthner axons on the same side of the spinal cord to have nonoverlapping axon collaterals. To test this, two different fluorophore-conjugated dextrans were electroporated into two separate Mauthner cells on the same side of the hindbrain in *des*^{b420} mutants. The positions of the labeled collaterals from the two different Mauthner cells were analyzed under confocal microscopy. We found that of 61 axon collaterals analyzed, 93% did not overlap with collaterals from the other labeled axon (Fig. 6, Table 3). In the small number of cases in which we did see overlap (two pairs), the collaterals might be contacting the same postsynaptic targets; although, even in these cases, they could be contacting different but adjacent postsynaptic neurons. These data suggest that supernumerary Mauthner axons in mutant larvae are forming synapses with largely nonoverlapping populations of spinal neurons and dividing their target territory. Together, these data are consistent with the hypothesis that each Mauthner cell in *des* mutants exerts less of an effect on downstream spinal neurons, and participation in the escape response is distributed among the population of Mauthner cells, thus maintaining a primarily normal escape response.

Discussion

The escape response in zebrafish is initiated by Mauthner cells, a single pair of large reticulospinal neurons. A mutation in the zebrafish gene *des*/*notch1a* results in a dramatic increase in the number of Mauthner cells without an equivalent increase in other neurons within the neural circuit that drives the escape response (Gray et al., 2001). Therefore, this mutation offers the unique opportunity to ask how the developing organism adapts to the presence of excess neurons and whether all of the cells are incorporated into the developing neural circuitry. Our analysis revealed that excess neurons are incorporated into the circuitry in a way that maintains the behavioral output. The more Mauthner cells that are present, the fewer collaterals there are per Mauthner axon. Moreover, Mauthner axons extending caudally in the same region of the spinal cord have very few collaterals that form in the same locations, strongly suggesting that Mauthner cells in *des* mutants are dividing their targets. These data reveal that there is plasticity in the formation of this vertebrate neural circuit, and the animal can adapt to the presence of excess cells in a manner that preserves the downstream behavior.

Mauthner cell and the escape response

Both experimental manipulations and genetic perturbations have been used to study the affect of cell loss on the escape-response circuit. Ablating Mauthner cells in wild-type animals causes a serious diminution of the tail-elicited escape response, whereas the head-elicited escape appears unchanged, suggesting that the Mauthner cell is the principal interneuron mediating the

Table 1. Escape response performance in wild-type and *des*^{b420} mutant larvae

		Latency to response[a] (msec)	Peak angular velocity[b] (°/msec)	Peak turn duration[b] (msec)	Peak turn angle[b] (°)
Wild-type	Heads	6.13 ± 0.15	22.55 ± 0.45	12.13 ± 0.30	201.35 ± 3.30
	Tails	11.0 ± 0.27	21.40 ± 0.43	8.97 ± 0.10	122.82 ± 3.32
des^{b420}	Heads	6.81 ± 0.24	21.47 ± 0.75	12.72 ± 0.27	175.09 ± 4.30
	Tails	10.92 ± 0.33	19.51 ± 0.56	10.83 ± 0.31	126.53 ± 3.11

Kinematic parameters were analyzed and compared using ANOVA. Turn duration was defined as the time from initiation of response to peak turn angle. Data are reported as mean ± SE.

[a]Three dpf homozygous mutants ($n = 6$) and wild-type siblings ($n = 4$).

[b]Five dpf homozygous mutants ($n = 6$) and wild-type mutants ($n = 5$).

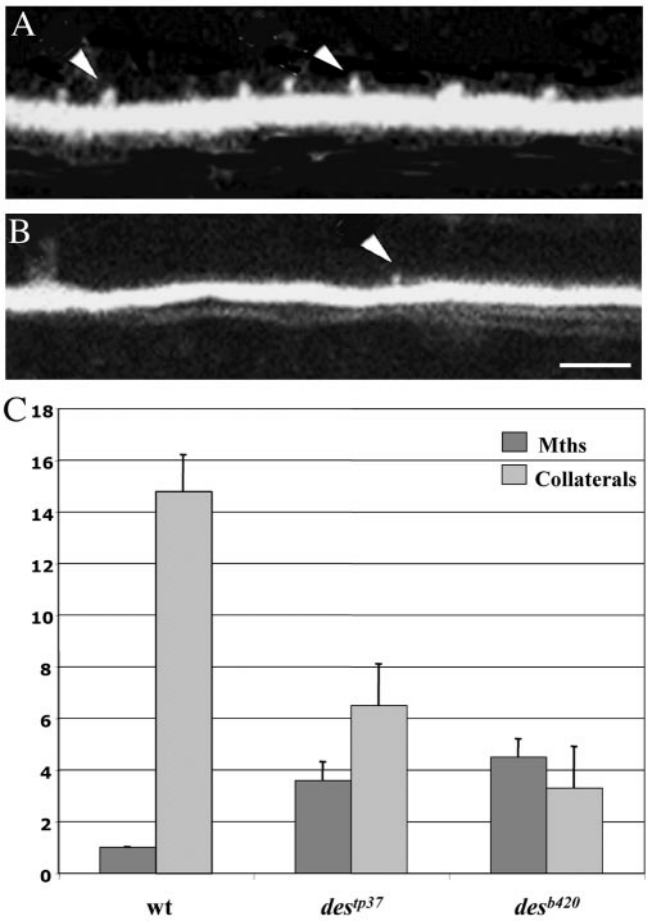

Figure 5. The number of collaterals per Mauthner axon is dramatically decreased in *des* mutants. *A*, *B*, Four dpf wild-type (*A*), *des*^{b420} (*B*), and *des*^{tp37} larvae were back-labeled from the caudal spinal cord with lysinated rhodamine dextran. The number of axon collaterals was quantitated over a three spinal cord hemisegment region in the midtrunk, and the number of Mauthner cells was counted under transmitted light (*C*). Arrowheads denote axon collaterals. Scale bar, 5 μm.

tail-elicited response (Liu and Fetcho, 1999). Additionally, in the zebrafish *space cadet*, mutant spiral fibers fail to contact Mauthner cells, resulting in aberrant escape behavior revealing a critical role for these cells in modulating the escape response (Lorent et al., 2001). Thus, the Mauthner cell and modulation of the Mauthner cell are essential for the tail-elicited escape behavior, and Mauthner cell loss cannot be compensated by other reticulospinal neurons involved in the escape response (i.e., MiD3cm and MiD2cm). However, our work indicates that an increase in the number of Mauthner cells neither strongly enhances nor diminishes the escape response.

Fish and premetamorphic amphibians have only a single, large, fast-conducting Mauthner cell that initiates the escape response. However, a similar response in mammals is primarily mediated by a population of 20–60 "giant neurons" in the caudal pontine-reticular formation in the brainstem (Lingenhohl and Friauf, 1992, 1994; Yeomans and Frankland, 1995). The question in terms of the construction of neuronal circuitry is whether the use of a single large cell, as opposed to several smaller cells, is advantageous for this crucial behavior. We focused primarily on the motor performance, the output side of the escape circuit, in mutant fish. Our data indicate that altering the number of cells has no dramatic affect on the motor output in the behavior. We did not explore the sensory side in as much detail, because it is more difficult to approach. The presence of extra cells might generate severe problems with the ability to properly integrate different sensory modalities (vision, somatosensation, lateral line, audition) to produce an appropriately timed motor response. Such deficits in integration of different modalities on the sensory side might explain why fish with extra Mauthner cells have not been observed in natural populations.

Mauthner axon collaterals

Our data show that there is a relationship between the number of Mauthner cells and the number of collaterals per Mauthner axon. It remains to be determined how the number and distribution of Mauthner axon collaterals are regulated. It may be that a Mauthner cell is sensitive to the presence of other Mauthner cells. Whether this regulation occurs at the level of the Mauthner cell body or axon is unclear. Alternatively, target cells in the spinal cord may mediate regulation. It is possible that once a spinal neuron is innervated by a Mauthner axon, it is bypassed by other Mauthner axons. On the basis of our data, we would predict that individual Mauthner cells in *des* mutants would have decreased output caused by their decreased numbers of axon collaterals compared with wild types. One way to test this idea would be to eliminate Mauthner cells and examine performance changes. We tried to laser ablate all but one Mauthner cell in *des*^{b420} mutants to get the biggest possible behavioral effect. Unfortunately, the tight juxtaposition of the Mauthner cell bodies makes controlled removal of the cells using dye phototoxicity very difficult, rendering this experiment unfeasible. Therefore, our data are consistent with this hypothesis, although the difficulties with selective ablations precluded a direct assessment of the contribution of each of the cells to the behavior.

Homozygous *des* mutants have other defects that could potentially effect the formation of Mauthner axon collaterals. For example, *des* mutants have mispatterned somites and defects in axon guidance (van Eeden et al., 1996; Gray et al., 2001). They also have a slight increase in the number of dorsal root ganglia sensory neurons, MiD3cm and RoL2 hindbrain interneurons, and a slight decrease in Rohon–Beard primary sensory neurons (Gray et al., 2001). However, both the tp37 and b420 alleles show these phenotypes to the same degree. The only significant differ-

Table 2. Axon collaterals in wild-type and *des* mutant larvae

Wild-type ($n = 10$)		*des*^{tp37} ($n = 10$)		*des*^{b420} ($n = 10$)	
Mauthner cells	Collaterals	Mauthner cells	Collaterals	Mauthner cells	Collaterals
1	14	5	5	4	7
1	16	3	6	5	4
1	15	4	5	3	4
1	13	3	8	5	0
1	13	5	4	4	3
1	12	4	5	6	2
1	18	2	12	3	4
1	14	3	8	5	0
1	16	4	6	5	3
1	17	3	6	5	0
1.0 ± 0.0	14.8 ± 1.4	3.6 ± 0.7	6.5 ± 1.6	4.5 ± 0.7	3.3 ± 1.6

Axons in 3 dpf wild-type, *des*^{tp37}, and *des*^{b420} mutant larvae were backfilled with lysinated rhodamine dextran at the posterior trunk level. Larvae were fixed at 4 dpf, and axon collaterals were counted over three spinal cord hemisegments under confocal microscopy. The number of Mauthner cells present on the side where the analyzed axon(s) originated was counted under transmitted light. Data are reported as mean ± 95% confidence interval. The decrease in axon collaterals observed in both *des*^{tp37} and *des*^{b420} mutants was statistically significant compared with wild types ($p < 0.0001$). In addition, the difference in axon collaterals between *des*^{tp37} and *des*^{b420} mutants was also significant ($p < 0.005$).

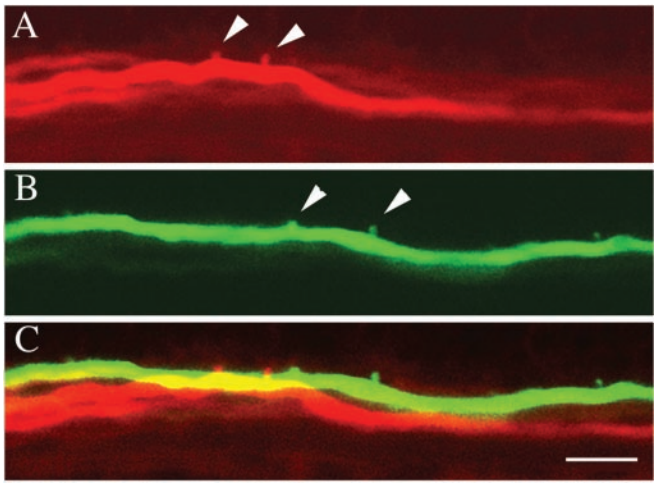

Figure 6. Collaterals from distinct Mauthner axons in *des*^{b420} mutants do not form in the same location. Two Mauthner cell bodies in *des*^{b420} mutants were electroporated with different fluorophores, and their axon collaterals were imaged at 6 dpf. One axon is shown in red (*A*), and the other is shown in green (*B*). The merged image (*C*) shows that the collaterals from the two axons do not form in the same location. Arrowheads denote collaterals. Scale bar, 10 μm

Table 3. Mauthner axon collaterals from distinct axons in *des*^{b420} mutants rarely form in the same position

	Collaterals		Overlapping collaterals
Fish	Red	Green	(pair)
A	3	5	0
B	2	6	0
C	2	7	0
D	4	7	0
	8	4	2
E	4	7	0

Two Mauthner cell bodies from 4 dpf *des*^{b420} larvae were electroporated with rhodamine or Far Red dextran, and their axons were analyzed over a three hemisegment length for collaterals at 6 dpf. Collaterals were considered overlapping if they were in the same position throughout the z-series. In fish D, collaterals were examined along two distinct axon regions.

ence between these two alleles is the number of Mauthner cells (Gray et al., 2001). Thus, the only phenotype in *des* mutants that consistently correlates to changes in Mauthner axon collateral numbers is the number of Mauthner cell bodies.

Our data show that all Mauthner cells in *des*^{b420} mutants are activated during an elicited escape response (Fig. 2). However, it is possible that different Mauthner cells in mutants contribute unequally to the response. For example, some Mauthner axons could have many collaterals and thus a stronger input onto spinal neurons, whereas other Mauthner axons could have fewer collaterals and less of an impact on spinal neurons. The totality of these responses would result in a normal escape response. However, the axon collateral data do not support this idea. Although there was variability in the number of axon collaterals counted, there was no clear subgrouping of axons having the wild-type number of collaterals and other axons having substantially fewer collaterals (Tables 2, 3). The one exception to this was an example in *des*^{tp37} in which there were only two Mauthner cells, and one of them had 12 collaterals over the three spinal cord hemisegment distance (Table 2). This number of collaterals was the smallest number seen in wild-type larvae (range, 12–18 collaterals per 3 hemisegments) and raises the possibility that when only two Mauthner cells are present, the number of collaterals approximates what is seen in wild-type larvae, where there is only one Mauthner cell. However, as soon as there are three Mauthner cells present, the number of collaterals decreases significantly (range, 4–8 collaterals per 3 hemisegments). Thus, there appears to be an overall decrease in the axon collateral number on each axon rather than a large decrease in collaterals on some axons.

Evolution of the escape response

Analysis of *des* mutants may yield insight into the evolution of the escape response. As mentioned above, a startle response in mammals analogous to the fish escape response is mediated by a population of 20–60 neurons in the caudal pontine-reticular formation that contacts spinal interneurons and motoneurons (Lingenhohl and Friauf, 1992, 1994; Yeomans and Frankland, 1995). Although individual axons have not been traced in mammals, it is thought that these cells distribute the activation of the stimulus to interneurons and motoneurons throughout the spinal cord. This is supported by the finding that neurotoxic lesions of the caudal pontine nucleus decreased the startle response (Koch et al., 1992). This scenario is similar to what we see in *des* mutants, in that Mauthner cells divide targets in the spinal cord. *des* mutants reveal that an evolutionary switch between one neuron and a population of neurons could be easily achieved by altering the number of target neurons contacted by each presynaptic cell as a way to maintain the integrity of the behavior. As a result, the animal can adapt to genetic changes, thus ensuring integrity of the behavior and survival. Such plasticity may have been important for the evolution of motor behaviors controlled by larger numbers of neurons.

References

Eaton RC, Lavender WA, Wieland CM (1981) Identification of Mauthner-initiated response patterns in goldfish: evidence from simultaneous cinematography and electrophysiology. J Comp Physiol 144:521–531.

Faber DS, Korn H (1978) Electrophysiology of the Mauthner cell: basic properties, synaptic mechanisms, and associated networks. In: Neurobiology of the Mauthner cell. New York: Raven.

Fetcho JR, Faber DS (1988) Identification of motoneurons and interneurons in the spinal network for escapes initiated by the Mauthner cell in goldfish. J Neurosci 8:4192–213.

Fetcho JR, O'Malley DM (1995) Visualization of active neural circuitry in the spinal cord of intact zebrafish. J Neurophys 73:399–406.

Gahtan E, O'Malley D (2003) Visually guided injection of identified reticulospinal neurons in zebrafish: a survey of spinal arborization patterns. J Comp Neurol 459:186–200.

Gray M, Moens CB, Amacher SL, Eisen JS, Beattie CE (2001) Zebrafish *deadly seven* functions in neurogenesis. Dev Biol 237:306–323.

Haas K, Javaherian WC, Li Z, Cline HT (2002) Single-cell electroporation for gene transfer *in vivo*. Neuron 29:583–591.

Holley SA, Julich D, Rauch GJ, Geisler R, Nusslein-Volhard C (2002) her1 and the Notch pathway function within the oscillator mechanism that regulates zebrafish somitogenesis. Development 129:1175–1183.

Kimmel CB, Session SK, Kimmel RJ (1981) Morphogenesis and synaptogenesis of the zebrafish Mauthner neuron. J Comp Neurol 198:101–120.

Kimmel CB, Hatta K, Metcalfe WK (1990) Early axonal contacts during development of an identified dendrite in the brain of the zebrafish. Neuron 4:535–545.

Koch M, Lingenhohl K, Pilz PKD (1992) Loss of the axoustic startle response following neurotoxic lesions of the caudal pontine reticular formation: possible role of giant neurons. Neuroscience 49:617–625.

Lingenhohl K, Friauf E (1992) Giant-neurons in the caudal pontine reticular-formation receive short latency acoustic input–an intracellular-recording and HRP-study in the rat. J Comp Neurol 325:473–492.

Lingenhohl K, Friauf E (1994) Giant neurons in the rat reticular formation: a sensorimotor interface in the elementary acoustic startle circuit. J Neurosci 14:1176–1194.

Liu KS, Fetcho JR (1999) Laser ablations reveal functional relationships of segmental hindbrain neurons in zebrafish. Neuron 23:325–335.

Lorent K, Liu KS, Fetcho JR, Granato M (2001) The zebrafish space cadet gene controls axonal pathfinding of neurons that modulate fast turning movements. Development 128:2131–2142.

Metcalfe WK, Mendelson B, Kimmel CB (1986) Segmental homologies among reticulospinal neurons in the hindbrain of the zebrafish larvae. J Comp Neurol 251:147–159.

Nissanov J, Eaton RC, DiDomenico R (1990) The motor output of the Mauthner cell, a reticulospinal command neuron. Brain Res 517:88–98.

O'Malley DM, Kao YH, Fetcho JR (1996) Imaging the functional organization of zebrafish hindbrain segments during escape behaviors. Neuron 17:1145–1155.

van Eeden FJM, Granato M, Schach U, Brand M, Furutani-Seiki M, Haffter P, Hammerschmidt M, Heisenberg CP, Jiang YJ, Kane DA, Kelsh RN, Mullins MC, Odenthal J, Warga RM, Allende ML, Wienberg ES, Nusslein-Volhard C (1996) Mutations affecting somite formation and patterning in the zebrafish, *Danio reiro*. Development 123:153–164.

Yeomans JS, Frankland PW (1995) The acoustic startle reflex: neurons and connections. Brain Res Brain Res Rev 21:301–314.

Zottoli SJ (1977) Correlation of the startle reflex and Mauthner cell auditory responses in unrestrained goldfish. J Exp Biol 66:243–254.